Use of converter furnace steel slag for bacteria removal in flow-through columns

Jin-Kyu Kang[a], Chang-Gu Lee[a], Jeong-Ann Park[a], Song-Bae Kim[b,*], Seungho Yu[c], Tae-Hun Kim[c]

[a]*Environmental Functional Materials & Biocolloids Laboratory, Seoul National University, Seoul 151-921, Republic of Korea*
[b]*Department of Rural Systems Engineering and Research Institute for Agriculture and Life Sciences, Seoul National University, Seoul 151-921, Republic of Korea*
Tel. +82 2 880 4587; Fax: +82 2 873 2087; email: songbkim@snu.ac.kr
[c]*Research Division for Industry and Environment, Korea Atomic Energy Research Institute, Jeongeup, Jeonbuk 580-185, Republic of Korea*

ABSTRACT

The aim of this study was to investigate the removal of bacteria (*Escherichia coli*) in flow-through columns (length = 10 cm; inner diameter = 2.5 cm) containing converter furnace steel slag and quartz sand. The X-ray fluorescence (XRF) analysis shows that calcium (Ca) and iron (Fe) were the major elements of the steel slag. The X-ray diffractometry (XRD) pattern indicates that hematite (Fe_2O_3), magnetite (Fe_3O_4), and dicalcium ferrite ($Ca_2Fe_2O_5$) were the major constituents of the steel slag. Results show that the percent removals of bacteria in the steel slag were 2.4–3.2 times greater than those of the sand. As the steel slag content increased from 0 to 100% in the mixture of steel slag and sand, the percent removal increased from 39.9 ± 2.7 to $97.3 \pm 0.1\%$. Results indicate that the steel slag was effective in the removal of bacteria. This could be attributed to iron oxides present in the steel slag, which play an important role of bacterial adhesion. Also, calcium oxide, which was released from the steel slag, could contribute to the removal of bacteria as bactericide. This study demonstrates that the steel slag has potential as a reactive media to remove bacteria from aqueous solution.

Keywords: Bacteria removal; Calcium oxide; Column experiment; Converter furnace steel slag; Iron oxide

1. Introduction

Iron/steel slags are produced in large quantities as by-products of iron/steel manufacturing processes. They are commonly used as road bed materials, cement additives, landfill cover materials, and contaminant adsorbents [1]. Iron/steel slags are classified into basic oxygen furnace steel slag (BOFSS) and blast furnace iron slag (BFIS). BFIS is primarily composed of silica (SiO_2) and alumina (Al_2O_3) along with calcium and magnesium oxides (CaO, MgO). BOFSS has a similar chemical composition to BFIS but has higher iron and manganese oxides contents (FeO, MnO). BOFSS is further divided into electric arc furnace steel slag and

*Corresponding author.

converter furnace steel slag, depending on the type of furnace from which it is generated [2].

Iron/steel slags have been used by several researchers to investigate the removal of various contaminants from aqueous solutions [3–5]. Sunahara et al. [6] used blast furnace slag to evaluate phosphate removal in synthetic wastewater using column experiments. Ahn et al. [7] used basic oxygen furnace slag as permeable reactive materials for arsenic removal in mine tailing leachate. Oh et al. [8] evaluated the efficiency of converter slag to remove organic/inorganic contaminants and heavy metals from landfill leachate. Park et al. [9] examined the mechanism and kinetics of Cr(VI) removal in blast furnace slag. These studies demonstrated that iron/steel slags are valuable industrial by-products, which can be used for contaminant removal from aqueous solutions. To our knowledge, however, studies related to the removal of microorganisms by iron/steel slags are scarce, including only one study by Stimson et al. [10] to evaluate the removal of bacteriophage in basic oxygen furnace slag using batch and column experiments. Further experiments are needed to improve our knowledge regarding the performance of slag materials in pathogen removal.

The aim of this study was to investigate the removal of bacteria from aqueous solution using converter furnace steel slag. The characteristics of the steel slag were elucidated using X-ray fluorescence spectrometer (XRF), X-ray diffractometry (XRD), Field emission scanning electron microscopy, energy dispersive X-ray spectrometry, and nitrogen gas adsorption–desorption analysis. Laboratory experiments were performed in columns under flow-through condition, and the breakthrough curves (BTCs) of bacteria were obtained by monitoring effluent.

2. Materials and methods

2.1. Bacteria and culture preparation

Escherichia coli ATCC 11,105 obtained from the Korea Culture Center for Microorganisms was used in the experiment. All glassware and materials used in this study were sterilized by autoclaving at 121°C and 17.6 psi for 20 min to prevent any interference by other microorganisms. Initially, the freeze-dried bacteria were revived in 250-mL Erlenmeyer flasks containing 100 mL of LB medium (tryptone 10 g, yeast extract 5 g, NaCl 5 g in one liter of deionized water) over a period of 84 h. Then, one milliliter of culture was transferred to a volume of 500 mL LB broth, and the bacteria were incubated over a period of 84 h at 30°C.

The suspension was centrifuged at 4°C and 10,000 rpm for 15 min. The supernatant was removed and replaced with deionized water to prevent growth of the bacteria. Then, the diluted bacteria were centrifuged again under the same conditions. The centrifuged bacteria were washed three times with deionized water and resuspended in deionized water to use [11].

2.2. Porous media

The steel slag (Ecomaister Co., Incheon, Korea) and quartz sand (Jumunjin Silica, Jumunjin, Korea) were used in the experiments. Mechanical sieving was conducted with US Standard Sieves No. 30 and No. 40 (grain size = 0.43–0.60 mm) to prepare the steel slag and sand for the experiments. The characteristics of the steel slag and sand were examined by various methods. Before analyses, both the steel slag and sand were washed twice using deionized water to remove impurities on the surface, and wet filter materials were autoclaved for 15 min at 17.6 psi, cooled to room temperature, and oven-dried at 105°C for 1–2 days. The chemical compositions of the steel slag and sand were investigated using an X-ray fluorescence spectrometer (XRF, S4 pioneer, Bruker, Germany). The mineralogical and crystalline structural properties of the steel slag were examined using X-ray diffractometry (XRD, D8 Advance, Bruker, Germany) with a CuKα radiation of 1.5406 Å at a scanning speed of 0.6°/s. N_2 adsorption–desorption experiments were performed using a surface area analyzer (BELSORP-max, BEL Japan Inc., Japan) to determine the specific surface area, average pore diameter, and total pore volume of the steel slag. Field emission scanning electron microscopy (FESEM) analysis was performed using a field emission scanning electron microscope (Supra 55VP, Carl Zeiss, Germany) to observe the surfaces of the steel slag. Elemental composition was determined by energy dispersive X-ray spectrometry (EDS) (XFlash 4000; Bruker AXS Microanalysis, Berlin, Germany) combined with an electron microscope at an accelerating voltage of 15 kV. X-rays were collected with a detector fixed at a take-off angle of 35°. Region analysis and color mapping were performed on the steel slag.

2.3. Column experiments

Column experiments were performed using a Plexiglas column (inner diameter = 2.5 cm, column length = 10 cm) packed with the steel slag and sand. For column experiments, a column was packed for

each experiment with steel slag (mass of porous media = 113.3 ± 0.9 g; bulk density = 2.31 ± 0.02 g cm^{-3}; porosity = 0.31 ± 0.04) and quartz sand (mass of porous media = 77.5 ± 2.1 g; bulk density = 1.54 ± 0.06 g cm^{-3}; porosity = 0.40 ± 0.02) by the tap-fill method. Prior to the experiments, the packed column was flushed upward using a HPLC pump (Series II pump, Scientific Systems Inc., State College, PA, USA) operating at a rate of 0.3 mL min^{-1} using 8 bed volumes of solution (1 mM NaCl + 0.1 mM NaHCO$_3$, pH = 6.6) until steady-state flow conditions were established by checking the effluent solution reaching the constant volume. Then, bacteria solution of $\sim10^9$ colony forming unit (CFU) mL^{-1} was introduced downward for 30 min to the packed column at the same flow rate. Portions of the effluent were collected using an autocollector (Retriever 500, Teledyne, City of Industry, CA, USA) at regular intervals. Effluent samples were analyzed for bacterial concentration along with electrical conductivity (EC) and pH. Bacterial concentrations were determined by colony counts from the LB agar plates. EC was measured with an EC probe (815PDL, Istek, Korea) and pH with a pH probe (9107BN, Orion, USA). In addition, the column experiments were performed at various slag contents and flow rates. The experimental conditions are provided in Table 1.

2.4. Data analysis

The one-dimensional bacteria transport in porous media can be described as [12]:

$$\frac{\partial C}{\partial t} = D\frac{\partial^2 C}{\partial x^2} - v\frac{\partial C}{\partial x} - kC \tag{1}$$

where C is the bacterial concentration in the aqueous phase (CFU mL^{-1}), D is the hydrodynamic dispersion coefficient for bacteria (cm^2 min^{-1}), v is the bacterial velocity (cm min^{-1}), and k is the removal rate coefficient (min^{-1}). Parameters in the transport models were obtained by fitting the CXTFIT code [13] to the BTCs of bacteria. The percent removal (Re) of bacteria was quantified by the following equation:

$$Re = \left(1 - \frac{\int_0^\infty C dt}{C_0 t_0}\right) \times 100(\%) \tag{2}$$

Table 1
Experimental conditions and results for bacteria removal in columns packed with converter furnace steel slag and quartz sand

Ex.	Porous media	Flow rate (mL min^{-1})	EBCT (min)	pH$_{eff}$	EC$_{eff}$ (μS cm^{-1})	Re (%)	v (cm min^{-1})	D (cm^2 min^{-1})	k (min^{-1})	D_a	R^2
1a	Steel slag 100%	0.3	44.9	10.4 ± 0.1	249.1 ± 7.4	97.4	0.224	0.188	0.085	3.79	0.90
1b	Steel slag 100%	0.3	44.9	10.3 ± 0.1	251.6 ± 4.9	97.2	0.221	0.188	0.083	3.76	0.95
2a	Steel slag 100%	0.6	22.5	9.9 ± 0.1	217.8 ± 4.3	88.1	0.355	0.628	0.099	2.79	0.96
2b	Steel slag 100%	0.6	22.5	10.0 ± 0.1	221.8 ± 3.2	84.8	0.348	0.648	0.097	2.79	0.98
3a	Sand 100%	0.3	66.7	6.6 ± 0.1	141.2 ± 2.7	41.8	0.140	0.030	0.009	0.64	0.99
3b	Sand 100%	0.3	66.7	6.2 ± 0.2	134.1 ± 2.0	38.0	0.157	0.045	0.010	0.64	0.99
4a	Sand 100%	0.6	33.4	6.4 ± 0.1	132.5 ± 0.9	22.7	0.314	0.139	0.014	0.45	0.99
4b	Sand 100%	0.6	33.4	6.5 ± 0.1	134.6 ± 1.5	31.9	0.303	0.100	0.017	0.56	0.99
5a	Steel slag 75% + sand 25%	0.3	50.3	8.9 ± 0.3	204.6 ± 16.4	80.6	0.167	0.142	0.034	2.04	0.94
5b	Steel slag 75% + sand 25%	0.3	50.3	9.3 ± 0.3	191.9 ± 7.0	88.1	0.169	0.127	0.038	2.25	0.95
6a	Steel slag 50% + sand 50%	0.3	55.9	8.6 ± 0.4	191.9 ± 10.7	74.6	0.160	0.219	0.029	1.81	0.90
6b	Steel slag 50% + sand 50%	0.3	55.9	8.1 ± 0.2	172.5 ± 6.4	79.3	0.163	0.239	0.030	1.84	0.99
7a	Steel slag 25% + sand 75%	0.3	61.6	6.9 ± 0.1	148.0 ± 2.9	57.3	0.152	0.064	0.022	1.45	0.98
7b	Steel slag 25% + sand 75%	0.3	61.6	7.1 ± 0.1	151.5 ± 3.4	67.0	0.151	0.058	0.024	1.59	0.99

EBCT = empty bed contact time; EC = electrical conductivity; Re = percent removal; v = bacterial velocity; D = hydrodynamic dispersion coefficient for bacteria; k = removal rate coefficient; D_a = Damköhler number; R^2 = coefficient of determination.
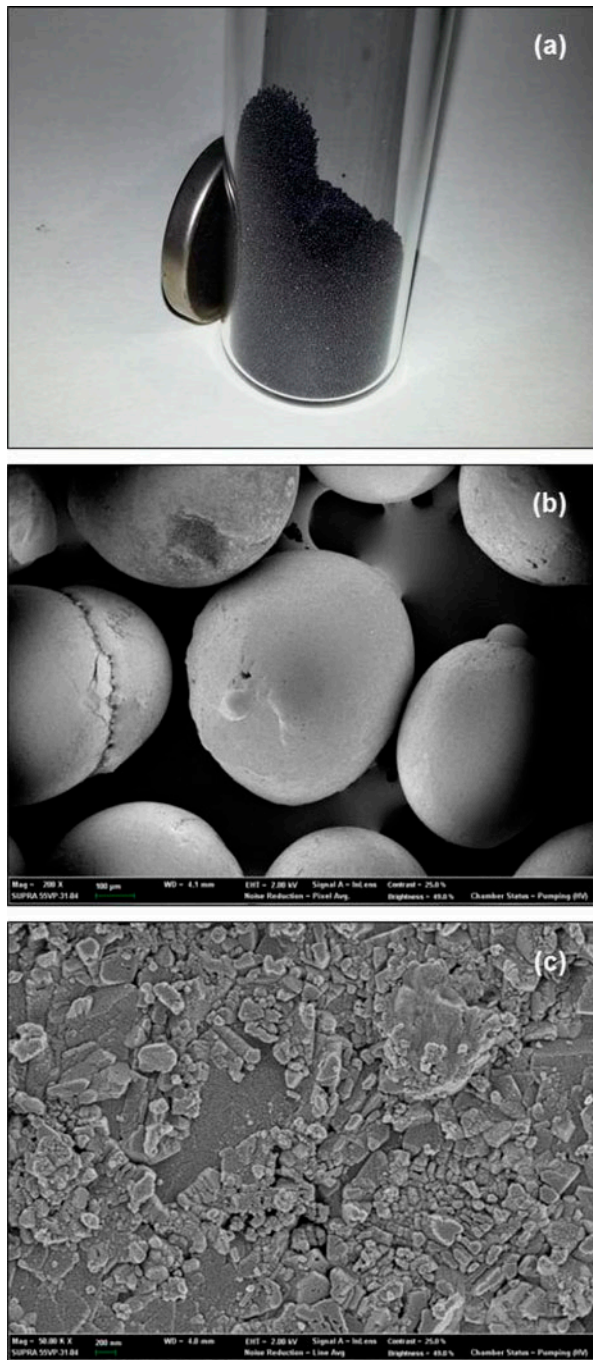
Fig. 1. Converter furnace steel slag used in the experiments: (a) digital image; (b) field emission scanning electron micrograph (FESEM, bar = 100 μm); (c) FESEM (bar = 200 nm).

where C_0 is the initial concentration of the bacteria in the synthetic solution, and t_0 is the duration of bacteria injection (injection time).

Table 2
Chemical compositions of converter furnace steel slag and quartz sand obtained from XRF analysis

	Chemical compositions (weight%)					
	SiO_2	Al_2O_3	CaO	MgO	Fe_2O_3/ FeO	Others
Converter furnace steel slag	10.3	2.0	40.7	8.8	25.1	13.1
Quartz sand	82.3	11.1	–	–	0.66	5.94

3. Results and discussion

3.1. Characteristics of the steel slag

The digital and FESEM images of the steel slag are shown in Fig. 1. The steel slag had a black color with a magnetic property (Fig. 1(a)). Also, it had microsphere shape with rough surfaces (Fig. 1(b) and (c)). The chemical compositions of the steel slag and sand obtained from the XRF analysis are presented in Table 2. The steel slag was mainly composed of CaO (40.7%) and Fe oxides (25.1%) as well as SiO_2, MgO, Al_2O_3, and MnO, whereas the sand of SiO_2 (82.3%), Al_2O_3 (11.1%), and other. The EDS patterns (Fig. 2) also indicate that Ca and Fe were the major elements of the steel slag with the weight% of Ca and Fe being 24.91 and 12.4%, respectively. Color mapping was performed to visualize the spatial distribution of Ca and Fe on the steel slag (Fig. 3). Ca was colored as yellow–green (Fig. 3(b) and (d)), whereas Fe was visualized as blue (Fig. 3(c) and (d)). The XRD analysis demonstrated that srebrodolskite (dicalcium ferrite, $Ca_2Fe_2O_5$), magnetite (Fe_3O_4), and hematite (Fe_2O_3)
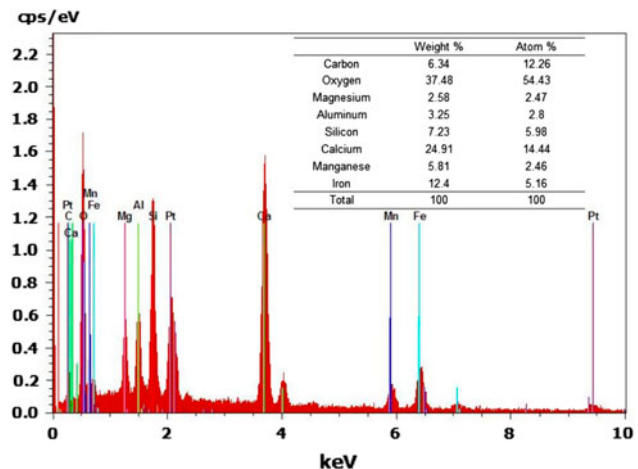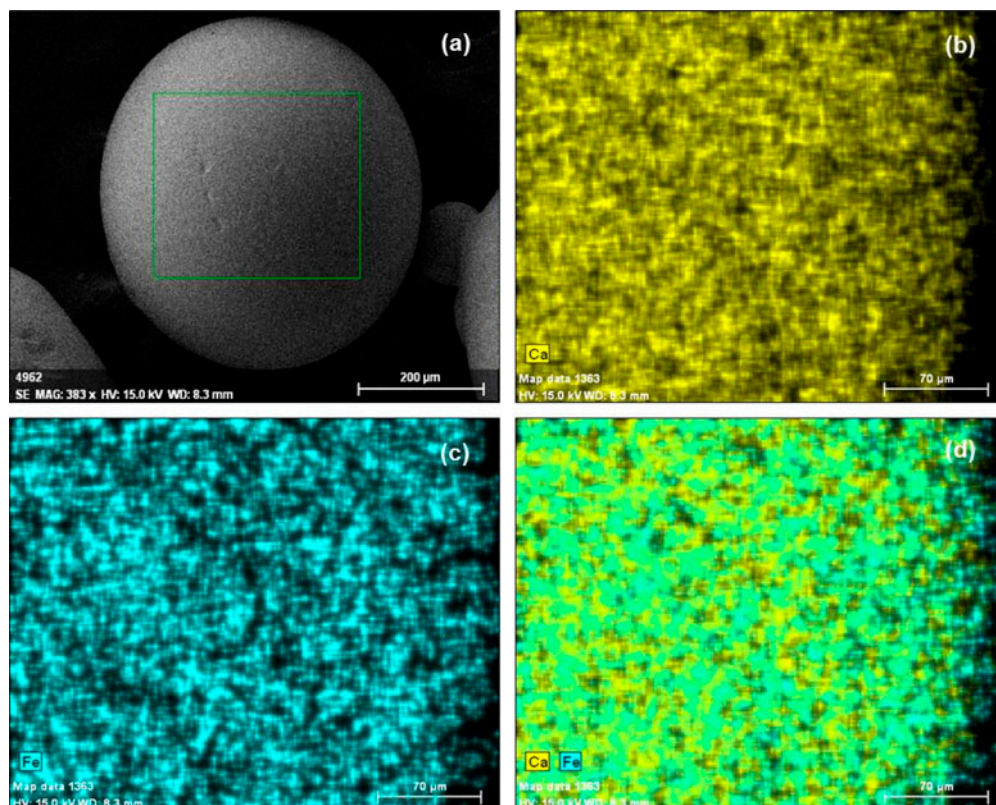

Fig. 2. EDS of converter furnace steel slag.

Fig. 3. Color mapping of converter furnace steel slag: (a) FESEM image of the steel slag (bar = 200 μm); (b) calcium (Ca) map; (c) iron (Fe) map; (d) overlay of the secondary electron image, Ca map, and Fe map.

were the major constituents of the steel slag (Fig. 4). From N_2 adsorption–desorption analysis, the BET surface area of the steel slag was $0.198 \, m^2 g^{-1}$ with total pore volume of $3.82 \times 10^{-4} \, cm^3 g^{-1}$ and average pore diameter of 7.70 nm.

3.2. Bacteria removal by the steel slag

The bacterial BTCs obtained from the experiments in the steel slag (100%) and sand (100%) columns at
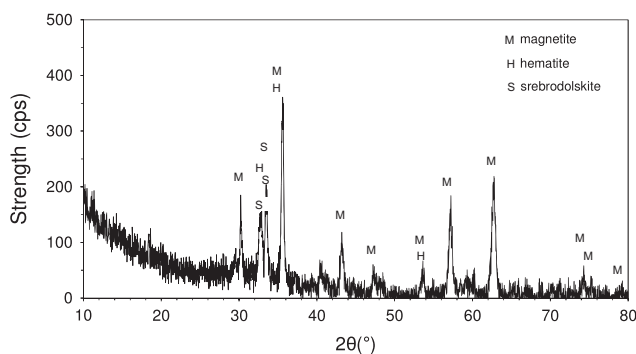
Fig. 4. XRD pattern of converter furnace steel slag.

the flow rates of 0.3 and $0.6 \, mL \, min^{-1}$ are presented in terms of time vs. relative concentration in Fig. 5. The experimental conditions are provided in Table 1. In the steel slag, the BTCs at $0.3 \, mL \, min^{-1}$ Fig. 5(1) had the relative peak concentrations of 0.02 (Ex. 1a and b), whereas the BTCs at $0.6 \, mL \, min^{-1}$ Fig. 5(2) had the peak concentrations of 0.07–0.09 (Ex. 2a and b). In the sand, the BTCs at $0.3 \, mL \, min^{-1}$ Fig. 5(3) had the peak concentrations of 0.37–0.38 (Ex. 3a and b), whereas the BTCs at $0.6 \, mL \, min^{-1}$ Fig. 5(4) had the peak concentrations of 0.41–0.43 (Ex. 4a and b).

The percent removals of bacteria in the steel slag and sand are shown in Fig. 6(a). At $0.3 \, mL \, min^{-1}$, the percent removal in the steel slag (Ex. 1) was $97.3 \pm 0.1\%$, which was 2.4 times greater than that $(39.9 \pm 2.7\%)$ of the sand (Ex. 3). The percent removal in the steel slag at $0.6 \, mL \, min^{-1}$ (Ex. 2) was $86.5 \pm 2.3\%$, whereas the percent removal in the sand at the same flow rate (Ex. 4) was $27.3 \pm 6.5\%$, which was 3.2 times smaller than that of the steel slag. From Fig. 6(a), the effect of flow rate on the percent removal could be observed. As the flow rate increased from 0.3 to $0.6 \, mL \, min^{-1}$, the percent removal in the steel slag decreased from 97.3 to 86.5%. Also, the percent
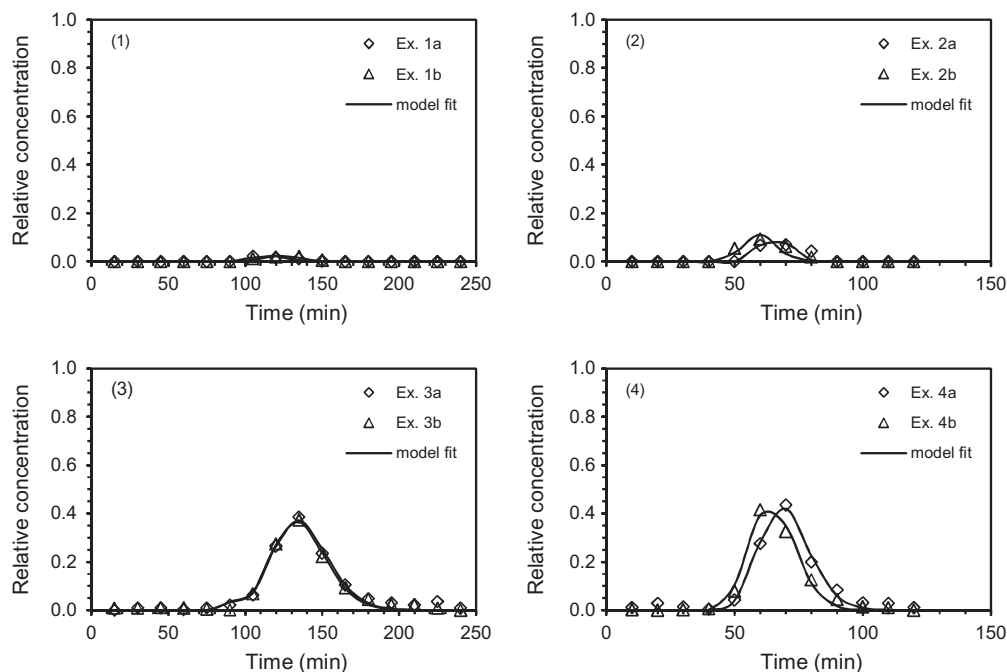
Fig. 5. Bacterial BTCs and model fits obtained from the column experiments in the steel slag (100%) and sand (100%) columns under two different flow rates: (1) steel slag, flow rate = 0.3 mL min^{-1}; (2) steel slag, flow rate = 0.6 mL min^{-1}; (3) sand, flow rate = 0.3 mL min^{-1}; (4) sand, flow rate = 0.6 mL min^{-1}.

removal in the sand decreased from 39.9 to 27.3% with an increase of flow rate. This result could be explained by the fact that the contact time between bacteria and porous media decreases as the flow rate increases. The empty bed contact time (EBCT) in the steel slag decreased from 45.0 to 22.5 min with increasing flow rate from 0.3 to 0.6 mL min^{-1}. In the sand, the EBCT decreased from 66.7 to 33.4 min with increasing flow rate.

The effect of the flow rate on the removal of bacteria could also be observed by plotting the Damköhler number (D_a) as a function of the flow rate (Fig. 6(b)). The value of D_a can be calculated from the removal rate coefficient (k) using the following relationship ($D_a = kL/v$, where L = column length and v = bacterial velocity). Note that D_a is used in the plotting instead of k because the interference of the bacterial velocity (v) on the removal rate coefficient (k) with time-scale effect during parameter estimation. Kim et al. [14] reported that a dimensionless parameter (D_a) should be used in order to interpret the column experimental data correctly if the rate coefficients show time-dependent characteristics. As shown in Fig. 6(b), the average value of D_a in the steel slag decreased from 3.78 to 2.79 with increasing flow rate from 0.3 to 0.6 mL min^{-1}. Also, the average value of D_a in the sand decreased from 0.66 to 0.50 with increasing flow rate. In contrast to D_a, the value of k increased with

increasing flow rate due to time-dependent characteristics (see Table 1). It is reasonable that the percent removal should decline with an increase of flow rate due to a decrease in contact time between bacteria and porous media.

The BTCs in the columns containing various contents of the steel slag and sand (slag content = 75, 50, 25%) are given from Fig. 7. The experimental conditions are summarized in Table 1. The BTCs had the relative peak concentrations of 0.06–0.08 (Fig. 7(1)), 0.10–0.12 (Fig. 7(2)), and 0.20–0.27 (Fig. 7(3)), showing an increasing tendency with decreasing the steel slag content in the column. The effect of the steel slag content on the percent removal and removal rate coefficient (k) is presented in Fig. 8. The removal percent was dependent on the steel slag content, increasing from 39.9 to 97.3 with an increase in the steel slag content from 0 to 100% in the columns. The removal rate coefficient also increased from 0.010 to 0.084 min^{-1} with increasing the steel slag content.

The results indicate that the steel slag is effective in the removal of bacteria. This could be attributed to iron oxides present in the steel slag. As mentioned previously, iron oxides such as hematite and magnetite were the major constituents of the steel slag. It is well known that iron oxides could play a positive role in the removal of bacteria [15–23]. Mailloux et al. [24] have reported that in geochemical heterogeneous
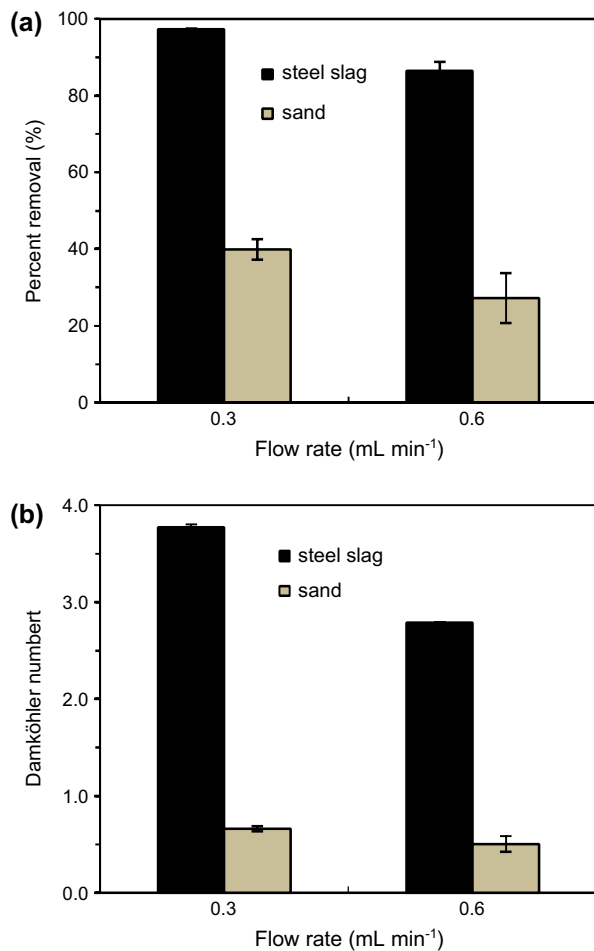
Fig. 6. Percent removal (a) and Damköhler number (b) of bacteria in the steel slag (100%) and sand (100%) columns under two different flow rates (0.3 and 0.6 mL min^{-1}).

aquifers, iron oxides provide surface charge heterogeneities, increasing the adhesion of bacteria to aquifer materials. Ams et al. [25] have shown that iron oxides coated on the sand provided the favorable sorption sites for bacteria, enhancing the removal of bacteria in the column.

In addition, calcium oxide (CaO) could contribute to the removal of bacteria. During the experiments, CaO of slag was released into solution when water was in contact with the steel slag [CaO + H$_2$O → Ca(OH)$_2$], resulting in the increment of pH and EC of the solution [10]. Note that in the steel slag column experiments (Ex. 1 and 2), the effluent pHs were 9.9–10.4 and the effluent EC values were 217.8–251.6 μS cm^{-1} (Table 1), which were 1.6–1.8 times larger than those (132.5–141.2 μS cm^{-1}) in the sand columns (Ex. 3 and 4). As presented in Table 1, as the slag content in the columns increased, the effluent pH increased because more CaO were released
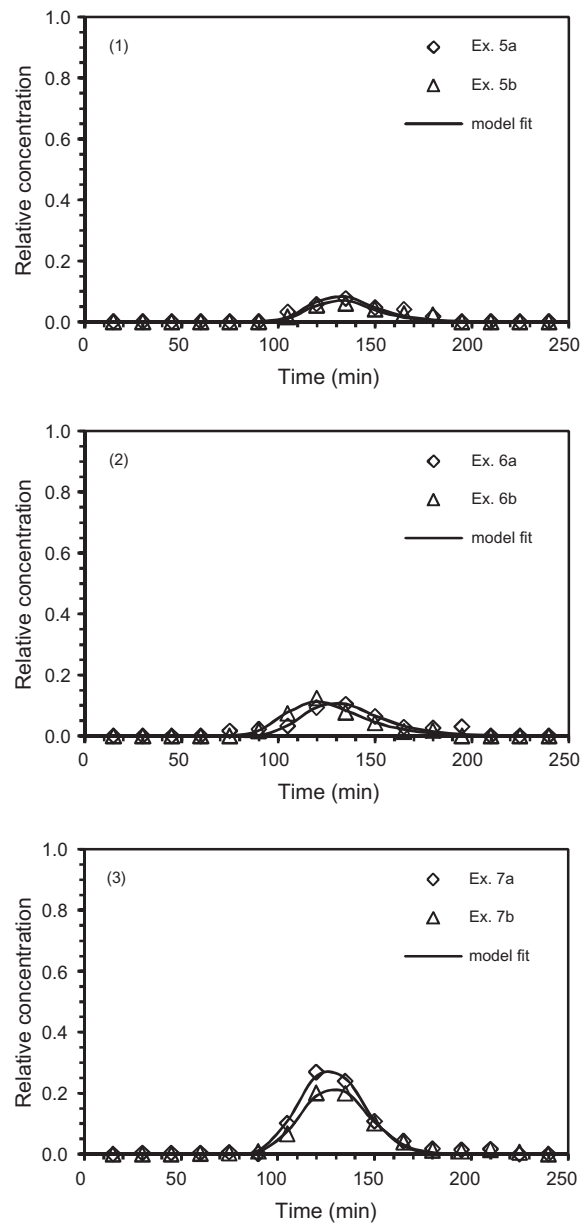

Fig. 7. Bacterial BTCs and model fits obtained from the column experiments in the mixture of the steel slag and sand (flow rate = 0.3 mL min^{-1}): (1) steel slag 75% + sand 25%; (2) steel slag 50% + sand 50%; (3) steel slag 25% + sand 75%.

from the columns. Also, the effluent EC increased as the slag content increased. Researchers have demonstrated that CaO could play a role of bactericide. Bae et al. [26] have suggested that the bactericidal activity of CaO on foodborne bacteria (*E. coli*, *Listeria monocytogenes*, *Salmonella typhimurium*) was related to the pH effect. They reported that the pH of the CaO solution increased to 11–12 as the CaO concentration increased [26]. Sawai [27] and Polprasert and Valencia [28]
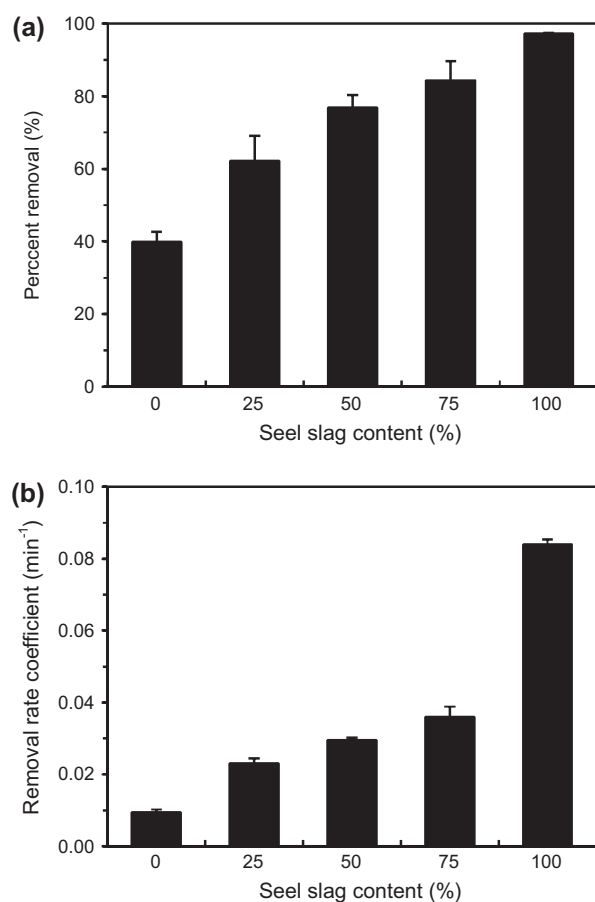
Fig. 8. Percent removal (a) and removal rate coefficient (b) of bacteria under various steel slag contents in the mixture of the steel slag and sand (flow rate = 0.3 mL min^{-1}).

The XRF analysis shows that calcium and iron were the major elements of the steel slag. The XRD pattern indicates that hematite, magnetite, and dicalcium ferrite were the major constituents of the steel slag. Results show that the percent removals of bacteria in the steel slag were greater than those of the sand. The percent removal increased as the steel slag content increased in the mixture of the steel slag and sand. Results indicate that the steel slag was effective in the removal of bacteria. This could be attributed to iron and calcium oxides present in the steel slag. This study demonstrates that the steel slag has potential as a reactive media to remove bacteria from aqueous solution. Further experiments are necessary to determine the optimal conditions for the slag filters to reach acceptable bacteria removal performances. In addition, more studies are required to examine both sorption and magnetic properties of the steel slag for contaminant removal and magnetic separation.

reported that the alkaline (OH$^-$) effect was the primary bactericidal mechanism of CaO. They also suggested that the bactericidal action of the oxygen radical generated from CaO might be the secondary mechanism [27,28]. Moya et al. [29] have shown the bactericidal effect for *E. coli* and *Micrococcus luteus* using glass powders containing CaO ranging from 15 to 20 weight percent. They reported that the Ca^{2+} leached from the glass powders could cause the depolarization of bacterial cell membranes and subsequent death [29]. It should be mentioned that in full scale application, the high pH in the effluent could be a problem if only the steel slag is used as porous media. It would be better to use the steel slag with other porous materials as mixtures or in sequence to reduce the high effluent pH.

4. Conclusions

In this study, the steel slag was used for the removal of bacteria under flow-through conditions.

References

[1] D.M. Proctor, K.A. Fehling, E.C. Shay, J.L. Wittenborn, J.J. Green, C. Avent, R.D. Bigham, M. Connolly, B. Lee, T.O. Shepker, M.A. Zak, Physical and chemical characteristics of blast furnace, basic oxygen furnace, and electric arc furnace steel industry slags, Environ. Sci. Technol. 34 (2000) 1576–1582.

[2] W. Cha, J. Kim, H. Choi, Evaluation of steel slag for organic and inorganic removals in soil aquifer treatment, Water Res. 40 (2006) 1034–1042.

[3] F.S. Zhang, H. Itoh, Iron oxide-loaded slag for arsenic removal from aqueous system, Chemosphere 60 (2005) 319–325.

[4] E. Nehrenheim, J.P. Gustafsson, Kinetic sorption modeling of Cu, Ni, Zn, Pb and Cr ions to pine bark and blast furnace slag by using batch experiments, Bioresour. Technol. 99 (2008) 1571–1577.

[5] J. Yang, S. Wang, Z. Lu, J. Yang, S. Lou, Converter slag-coal cinder columns for the removal of phosphorous and other pollutants, J. Hazard. Mater. 168 (2009) 331–337.

[6] H. Sunahara, W.M. Xie, M. Kayama, Phosphate removal by column packed blast furnace slag – I. Fundamental research by synthetic wastewater, Environ. Technol. 8 (1987) 589–598.

[7] J.S. Ahn, C.M. Chon, H.S. Moon, K.W. Kim, Arsenic removal using steel manufacturing byproducts as permeable reactive materials in mine tailing containment systems, Water Res. 37 (2003) 2478–2488.

[8] B.T. Oh, J.Y. Lee, J. Yoon, Removal of contaminants in leachate from landfill by waste steel scrap and converter slag, Environ. Geochem. Health 29 (2007) 331–336.

[9] D. Park, S.R. Lim, H.W. Lee, J.M. Park, Mechanism and kinetics of Cr(VI) reduction by waste slag generated from iron making industry, Hydrometallurgy 93 (2008) 72–75.

[10] J. Stimson, G.T. Chae, C.J. Ptacek, M.B. Emelko, M.M. Mesquita, R.A. Hirata, D.W. Blowes, Basic oxygen furnace slag as a treatment material for pathogens: contribution of inactivation and attachment in virus attenuation, Water Res. 44 (2010) 1150–1157.

[11] C.G. Lee, S.J. Park, H.C. Kim, Y.U. Han, S.B. Kim, Determination of bacterial mass recovery in iron-coated sand: Influence of ionic strength, J. Environ. Sci. Health A 43 (2008) 1108–1114.

[12] S.B. Kim, S.J. Park, C.G. Lee, H.C. Kim, Transport and retention of *Escherichia coli* in a mixture of quartz, Al-coated and Fe-coated sands, Hydrol. Process. 22 (2008) 3856–3863.

[13] N. Toride, F.J. Leij, M.Th. van Genuchten, The CXTFIT code for estimating transport parameters from laboratory or field tracer experiments, Research Report No. 137, US Salinity Laboratory, 1995.

[14] S.B. Kim, H.C. Ha, N.C. Choi, D.J. Kim, Influence of flow rate and organic carbon content on benzene transport in a sandy soil, Hydrol. Process. 20 (2006) 4307–4316.

[15] M.A. Scholl, A.L. Mills, J.S. Herman, G.M. Horngerger, The influence of mineralogy and solution chemistry on the attachment of bacteria to representative aquifer materials, J. Contam. Hydrol. 6 (1990) 321–336.

[16] M.A. Scholl, R.W. Harvey, Laboratory investigations on the role of sediment surface and groundwater chemistry in transport of bacteria through a contaminated sandy aquifer, Environ. Sci. Technol. 26 (1992) 1410–1417.

[17] E.P. Knapp, J.S. Herman, G.M. Hornberger, A.L. Mills, The effect of distribution of iron–oxyhydroxide grain coatings on the transport of bacterial cells in porous media, Environ. Geol. 33 (1998) 243–248.

[18] S.E. Truesdail, J. Lukasik, S.R. Farrah, D.O. Shah, R.B. Dickinson, Analysis of bacterial deposition on metal (hydr)oxide-coated sand filter media, J. Colloid Interf. Sci. 203 (1998) 369–378.

[19] J. Lukasik, Y.-F. Cheng, F. Lu, M. Tamplin, S.R. Farrah, Removal of microorganisms from water by columns containing sand coated with ferric and aluminum hydroxides, Water Res. 33 (1999) 769–777.

[20] P. Zhang, W.P. Johnson, T.D. Scheibe, K.-H. Choi, F.C. Dobbs, B.J. Mailloux, Extended tailing of bacteria following breakthrough at the narrow channel focus area, oyster, Virginia, Water Resour. Res. 37 (2001) 2687–2698.

[21] S.E. Silliman, R. Dunlap, M. Fletcher, M.A. Schneegurt, Bacterial transport in heterogeneous porous media: observations from laboratory experiments, Water Resour. Res. (2001) 2699–2707.

[22] J.W.A. Foppen, Y. Lien, J.F. Schijven, Effect of humic acid on the attachment of *Escherichia coli* in columns of goethite-coated sand, Water Res. 42 (2008) 211–219.

[23] S.B. Kim, S.J. Park, C.G. Lee, N.C. Choi, D.J. Kim, Bacteria transport through goethite-coated sand: effects of solution pH and coated sand content, Colloid. Surf. B 63 (2008) 236–242.

[24] B.J. Mailloux, M.E. Fuller, T.C. Onstott, J.A. Hall, H. Dong, M.F. DeFlaun, S.H. Streger, R.K. Rothmel, M. Green, D.J.P. Swift, J. Radke, The role physical, chemical, and microbial heterogeneity on the field-scale transport and attachment of bacteria, Water Resour. Res. 39 (2003) doi: 10.1029/2002WR001591.

[25] D.A. Ams, J.B. Fein, H. Dong, P.A. Maurice, Experimental measurements of the adsorption of *Bacillus subtilis* and *Pseudomonas mendocina* onto Fe–oxyhydroixde-coated and uncoated quartz grains, Geomicrobiol. J. 21 (2004) 511–519.

[26] D.H. Bae, J.H. Yeon, S.Y. Park, D.H. Lee, S.D. Ha, Bactericidal effects of CaO (scallop-shell powder) on foodborne pathogenic bacteria, Arch. Pharm. Res. 29 (2006) 298–301.

[27] J. Sawai, Quantitative evaluation of antibacterial activities of metallic oxide powders (ZnO, MgO and CaO) by conductimertic assay, J. Microbiol. Method 54 (2003) 177–182.

[28] C. Polprasert, L.G. Valencia, The inactivation of faecal coliforms and *Ascaris* ova in faeces by lime, Water Res. 15 (1981) 31–36.

[29] J.S. Moya, L. Esteban-Tejeda, C. Pecharromán, S.R.H. Mello-Castanho, A.C. da Silva, F. Malpartida, Glass powders with a high content of calcium oxide: a step towards a "green" universal biocide, Adv. Eng. Biomater. 13 (2011) B256–B260.